



## The dynamo effect/L'effet dynamo

# History and results of the Riga dynamo experiments

Agris Gailitis<sup>a</sup>, Gunter Gerbeth<sup>b</sup>, Thomas Gundrum<sup>b</sup>, Olgerts Lielausis<sup>a</sup>,  
Ernestis Platacis<sup>a</sup>, Frank Stefani<sup>b,\*</sup>

<sup>a</sup> Institute of Physics, University of Latvia, LV-2169 Salaspils 1, Latvia

<sup>b</sup> Forschungszentrum Dresden-Rossendorf, P.O. Box 510119, 01314 Dresden, Germany

Available online 29 August 2008

---

### Abstract

On 11 November 1999, a self-exciting magnetic eigenfield was detected for the first time in the Riga liquid sodium dynamo experiment. We report on the long history leading to this event, and on the subsequent experimental campaigns which provided a wealth of data on the kinematic and the saturated regime of this dynamo. The present state of the theoretical understanding of both regimes is delineated, and some comparisons with other laboratory dynamo experiments are made. **To cite this article:** A. Gailitis *et al.*, *C. R. Physique 9 (2008)*.

© 2008 Académie des sciences. Published by Elsevier Masson SAS. All rights reserved.

### Résumé

**Historique et résultats des expériences dynamo de Riga.** Le 11 novembre 1999, un mode propre magnétique auto-excité était détecté pour la première fois dans l'expérience dynamo au sodium liquide de Riga. Nous relatons le long historique qui a conduit à cet événement et présentons les campagnes expérimentales qui ont suivi et qui ont produit de très nombreuses données sur les régimes cinématique et saturé de cette dynamo. L'état actuel de compréhension théorique des deux régimes est esquissée et des comparaisons avec d'autres expériences dynamo sont fournies. **Pour citer cet article :** A. Gailitis *et al.*, *C. R. Physique 9 (2008)*.

© 2008 Académie des sciences. Published by Elsevier Masson SAS. All rights reserved.

**Keywords:** Dynamo; Magnetic field; Liquid sodium

**Mots-clés:** Dynamo ; Champ magnétique ; Sodium liquide

---

## 1. Introduction

It is widely believed that almost any flow of a conducting liquid will give rise to self-excitation of a magnetic field provided that, first, the flow topology is not too simple (e.g. a flow in one direction or a purely rotational flow) and, second, the so-called magnetic Reynolds number is large enough. This dimensionless number  $Rm = \mu_0 \sigma LV$ , which is defined as the product of the magnetic permeability  $\mu_0$  and the electrical conductivity  $\sigma$  of the fluid and the typical

---

\* Corresponding author.

E-mail addresses: [gailitis@sal.lv](mailto:gailitis@sal.lv) (A. Gailitis), [G.Gerbeth@fzd.de](mailto:G.Gerbeth@fzd.de) (G. Gerbeth), [Th.Gundrum@fzd.de](mailto:Th.Gundrum@fzd.de) (T. Gundrum), [mbroka@sal.lv](mailto:mbroka@sal.lv) (O. Lielausis), [platacis@sal.lv](mailto:platacis@sal.lv) (E. Platacis), [F.Stefani@fzd.de](mailto:F.Stefani@fzd.de) (F. Stefani).

length scale  $L$  and the typical velocity scale  $V$  of its flow, measures the ratio of diffusive time scale to kinematic time scale in the induction equation for the magnetic field  $\mathbf{B}$ :

$$\frac{\partial \mathbf{B}}{\partial t} = \nabla \times (\mathbf{v} \times \mathbf{B}) + \frac{1}{\mu_0 \sigma} \nabla^2 \mathbf{B} \quad (1)$$

While this number is large in many astrophysically relevant flows, simply due to their huge spatial extension, it requires significant effort to produce a flow with  $Rm \sim 10, \dots, 100$  in the laboratory. The simple reason for this is that the electrical conductivity of liquid metals, even in the optimum case of liquid sodium, does not exceed a value of  $10^7$  S/m, which leads to a product  $\mu_0 \sigma \sim 10$  s/m<sup>2</sup>. Hence, in order to get an  $Rm \sim 10$ , it requires a product of fluid dimension and flow velocity of  $VL \sim 1$  m<sup>2</sup>/s. It is this large number, in connection with the precautions that are indispensable for the safe handling of sodium, which had prevented dynamo experiments for a long time.

There are many possibilities to organize a dynamo-active flow in a vessel, and quite a number of them have been tried in experiment. By now, experimental dynamo science is completely international with strong activities in Latvia, Germany, France, US, and Russia. These attempts, only three of which were successful in showing dynamo action, have been summarized in a number of recent review papers [1–6], and some of them are also described in the present special issue. Therefore, in this paper we will restrict our attention to the Riga dynamo experiment, with only a few comparative side-views on other experiments.

## 2. The history of the Riga dynamo experiment

The idea of the Riga dynamo experiment originates from one of the simplest dynamo concepts that was investigated by Ponomarenko in 1973 [7]. The Ponomarenko dynamo consists of one conducting rigid rod which undergoes a spiral motion within – and in gliding contact with – a medium of the same conductivity that extends infinitely in the radial and axial directions. People working on planetary, stellar, or galactic dynamos might be sceptical about the physical relevance of such a system. The first answer to them is that this dynamo represents an “elementary cell” of a number of more complicated dynamos, and in this function it deserves particular attention in its own right. The second answer is that possibly some natural systems work in a similar manner as the Ponomarenko dynamo. One promising candidate is the “double helix nebula” which was detected recently in the outflow from the galactic centre [8]. The basic idea that cosmic jets could work as a Ponomarenko-like dynamo was already discussed in an early paper by Shukurov and Sokoloff [9].

Soon after its invention by Ponomarenko, the dynamo was further analyzed by Gailitis and Freibergs [10] who found a remarkably low critical magnetic Reynolds number for the convective instability of 17.7 (with the radius taken as the defining length scale). An essential step towards an experimental realization was the consideration of a straight back-flow concentric to the inner helical flow, which converts the convective instability into an absolute one [11].

Based on this early analytical and numerical work, a first experimental attempt was undertaken in 1986 by Gailitis et al. [12]. In contrast to the later Riga dynamo experiment, the central helical flow in this experiment was actualized by a spiral flow guide (the “helical labyrinth”) at the entrance of the flow. The main experimental result was the observation of a significant amplification of an externally applied magnetic field. Unfortunately, the experiment had to be stopped due to some construction problems leading to strong mechanical vibrations, and so it is not known if this dynamo would have been able to show self-excitation.

With this experience in mind, it was decided to change slightly the concept of the experiment by replacing the “helical labyrinth” by a propeller and some guiding blades, restricted to the inlet of the central tube. Later we will see that the lack of mechanical constraints along the 3 m distance from the propeller region to the bottom qualifies this dynamo as a markedly *fluid* dynamo, in which the saturation mechanism of the magnetic field strongly relies on the deformability of the velocity field. In addition to the concentric back-flow channel, a third cylinder with sodium at rest was attached in order to further reduce the critical  $Rm$  due to improved boundary conditions for the electric currents.

A good deal of work was devoted to the optimization of the geometry and the details of the flow structure. The main dimensions, i.e. length and the radii of the three cylinders were optimized in [13]. A further idea of optimization relied on the expectation that a flow with maximum helicity (at fixed kinetic energy) should represent a sort of optimum for dynamo action to occur. The calculus of variation for the corresponding problem in cylindrical geometry leads to Bessel functions of the zero and first order for the axial and the azimuthal velocities, respectively. It turned out that

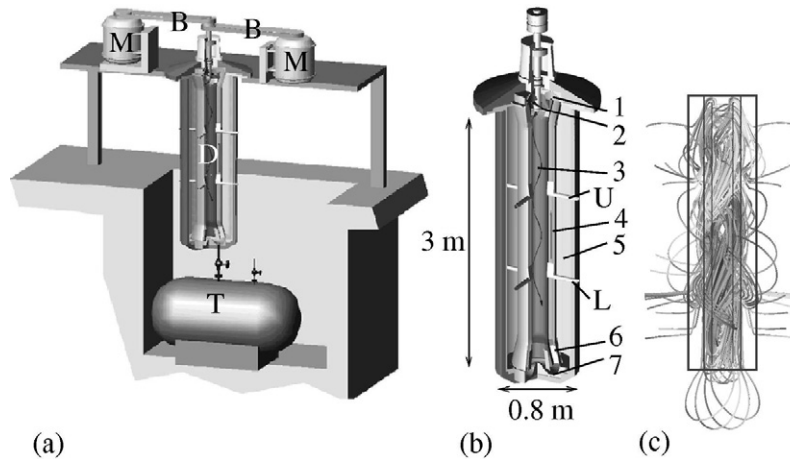


Fig. 1. The Riga dynamo experiment and its eigenfield. (a) Sketch of the Riga dynamo facility. M – Two 100 kW motors. B – Belts from the motors to the propeller shaft. D – Central dynamo module. T – Sodium tank. (b) Details of the central dynamo module. 1 – Upper bending region; 2 – Propeller; 3 – Central helical flow region; 4 – Return-flow region; 5 – Outer sodium region; 6 – Guiding vanes for straightening the flow in the return flow. 7 – Lower bending region. At approximately  $1/3$  (L) and  $2/3$  (U) of the dynamo height there are four ports for various magnetic field, pressure and velocity probes. (c) Simulated structure of the magnetic eigenfield in the kinematic regime.

radial flow profiles of this kind lead indeed to a minimum for the critical magnetic Reynolds number [14]. For people familiar with Taylor relaxation and the reversed field pinch [15], in which a turbulent plasma produces a magnetic field of the same Bessel function shape, this might appear as an intriguing duality of velocity optimization and magnetic-field self-organization.

Besides the general problems in setting up a large scale liquid sodium facility, the realization of the desired flow structure was a time-consuming process in particular. Most of the work was done by G. Will, M. Christen and H. Hänel at the Technical University of Dresden, where a 1:2 water dummy model of the Riga sodium facility was built and utilized for flow measurements and optimization [16]. While the propeller geometry was fixed at an early stage, much numerical and experimental effort was needed to find a configuration of pre- and post-propeller vanes suitable to shape the flow as close as possible to the desired Bessel function profiles.

Between 1995 and 1999, the dynamo facility was installed at the Institute of Physics in Salaspils, Latvia (actually, the name “Riga dynamo experiment”, which has been chosen for a better recognizability, is not fully correct, since Salaspils is an independent town 25 km eastward of Riga). The main components of the facility and the structure of the simulated (and experimentally widely confirmed) magnetic eigenfield are shown in Fig. 1.

After all preparations had been done, a first experimental campaign took place on 10–11 November 1999. Before an experiment starts, sodium is usually heated up to  $300\text{ }^{\circ}\text{C}$  and pumped slowly through the central module for about 24 hours in order to achieve good electrical contact between sodium and the internal stainless steel walls. It was planned to decrease the temperature to approximately  $150\text{ }^{\circ}\text{C}$  since the electrical conductivity and hence the magnetic Reynolds number increase with decreasing temperature. During this cooling-down process, some measurements of the amplification of an externally applied magnetic field were carried out [17,19,20]. Amplification factors up to 25 were identified, with a distinct resonance behaviour at such propeller rotation rates where the frequency of the applied field corresponds to the eigenfrequency of the dynamo. For almost all rotation rates the measured signal had only a single component with the frequency of the applied field. However, at the highest achieved propeller rotation rate of 2150 rpm, an additional exponentially increasing mode was identified with a frequency different from that of the externally applied field (see Fig. 2).

Due to some technical problems arising with the seal, this highest rotation rate had soon to be reduced to 1980 rpm, at which the external field was switched off. This allowed the observation of a pure eigenstate, which was already slowly decaying at this lowered rotation rate [17,18,20]. In hindsight it can be stated that the eigenfrequencies and growth rates measured at these two events fit perfectly into the many other data that were taken in later experimental campaigns. Hence 11 November 1999 marks the first observation of an exponentially growing eigenmode in a liquid metal dynamo experiment.

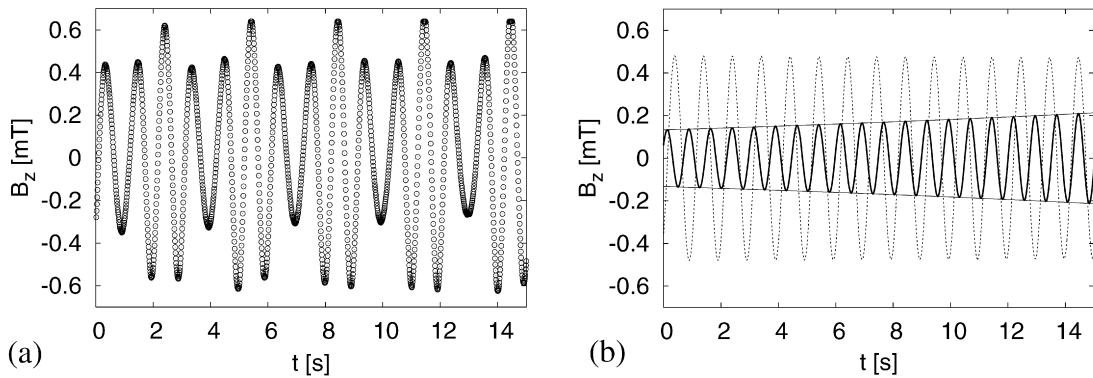


Fig. 2. (a) Axial magnetic field measured by a fluxgate sensor (situated close to the innermost wall) at the highest propeller rotation of 2150 rpm on 11 November 1999. (b) Decomposition of this signal into the amplified externally applied field (dotted line) and the exponentially increasing self-excited dynamo eigenmode (full line).

What was, however, not achieved in this first experimental campaign was the saturated regime of the dynamo in which the Lorentz forces resulting from the self-excited magnetic field reduce the amplitude and modify the structure of the flow velocity in such a way that the growth rate drops down to zero. To observe this saturated state took another 8 months in which a new seal had to be installed. Then, in July 2000, four runs were carried out, partly with, partly without externally applied magnetic fields, which provided a first stock of growth rate, frequency, and spatial structure data of the magnetic eigenfield [21].

A further step towards the detailed determination of the magnetic eigenfield was done in June 2002, when several lances with radially spaced Hall sensors were inserted into the dynamo module.

A somehow frustrating story was the attempt to measure flow velocities in a direct manner. This was, for the first time, tried in February 2003 and reiterated in the July 2003 and May 2004 campaigns, when three ultrasonic transducers were installed at the outer wall in order to measure the velocity in the outermost cylinder of the dynamo. Note that there is no mechanical forcing of the sodium in this outer cylinder, and any significant flow there can only result from the Lorentz forces due to the magnetic eigenfield. This flow structure was numerically estimated to be a main rotation with a velocity of the order of 1 m/s, and a poloidal flow in the form of a double vortex. This flow structure was experimentally confirmed during some runs in the May 2004 campaign, while we failed to study it in more details in further runs. The reason for this failure is not completely clear: it seems that, after some short initial phase in which data can be collected, the Lorentz force induced flow stirs up a lot of oxides in the outer cylinder which then accumulate at the interfaces of the ultrasonic transducers that may act as cold traps.

Another novelty of the May 2004 campaign was the measurements of pressure data in the inner dynamo channel by a piezoelectric sensor that was flash mounted at the innermost wall. These measurements provided not only the expected  $f^{-7/3}$  behaviour of the pressure fluctuations [22], but also the velocity modes at the double and the quadruple of the eigenfrequency of the dynamo which result from the non-axisymmetric parts of the Lorentz forces.

Another attempt to measure velocities in a direct way was undertaken in February/March 2005 when a stainless-steel permanent magnet probe for the determination of flow induced electric potentials was installed. In principle, this probe has provided data on the velocity. However, it was not trivial to disentangle the axial and the azimuthal velocity components from the obtained signals. What was also new in the February/March 2005 campaign was the installation of two traversing rails with Hall sensors moving in axial direction outside the dynamo and induction coils moving in radial direction within the dynamo module. These traversing sensor rails allowed for the detailed determination of the spatial structure of the magnetic eigenfield, the results of which will be published elsewhere.

Fig. 3 shows the axial magnetic field measured by induction coils inside the upper and the lower port close to the innermost wall during the last run on 1 March 2005. This figure might serve as an example on how the magnetic field can be switched on and off at will, and on how its amplitude depends on the propeller rotation rate. Comparing Figs. 3(a) and 3(b), a peculiarity of this dependence becomes visible. Whereas at the upper sensor (Fig. 3(b)) the field amplitude increases from 27 mT for 2000 rpm to 120 mT for 2500 rpm, at the lower sensor (Fig. 3(a)) the corresponding increase is only from 24 mT to 65 mT. This is a clear indication for a drastic change of the field

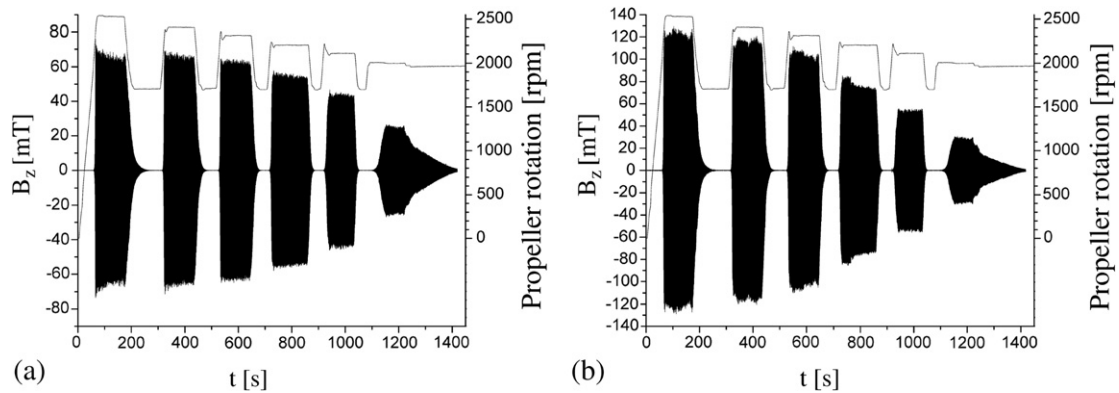


Fig. 3. Axial magnetic field and propeller rotation rate during the run 6 of the February/March 2005 campaign, measured by induction coils within the lower (a) and upper (b) port, close to the innermost wall where the axial magnetic field has its maximum.

dependence in axial direction with increasing supercriticality of the dynamo, which in turn mirrors a significant change of the axial dependence of the flow.

The most recent campaign was undertaken in July 2007, after which the outworn gliding ring seal for the propeller shaft was replaced by a magnetic coupler which had been designed and produced by SERAS-CNRS in Grenoble. After a few successful runs had been done with this magnetic coupler, the experiment had to be stopped due to fact that the belts between the motors and the propeller shaft were broken.

### 3. Summary of main results

The most significant number for the qualification of a dynamo is the growth rate of the magnetic field eigenmode. In the subcritical regime, this negative number can either be obtained after switching off an externally applied magnetic field or by lowering the propeller rotation rate from supercritical to subcritical and tracing again the following exponential decay of the eigenfield. When the dynamo is driven into the supercritical state, there are typically a few seconds during which the field is still weak enough so that the dynamo can be considered as a kinematic one. Since the Riga dynamo has a complex eigenvalue, there is also a rotation frequency of the eigenfield which can easily be determined both in the kinematic and in the saturated regime.

During the eight experimental campaigns, plenty of growth rate and frequency measurements were carried out. When scaled appropriately by the temperature dependent conductivity of sodium, both quantities turned out to be reproducible over the years. Only a slight change appeared, starting with the June 2002 campaign when a lance with sensors was inserted into the central helical flow leading to a slight additional braking of the flow and a corresponding slight decrease of the growth rate.

In Fig. 4, the temperature corrected measurements for the growth rate (Fig. 4(a)) and the frequency (Fig. 4(b)) are shown in comparison with the corresponding numerical results. The numerical curves in the kinematic regime were obtained with the 2D solver [14,27] and were corrected for the slight effect of the lower conductivity of the stainless steel walls that was estimated separately by a 1D solver. As for the saturation regime we have tried to identify the most important back-reaction effect within a simple one-dimensional model [19,26]. While the axial velocity component has to be rather constant from top to bottom due to mass conservation, the azimuthal component  $v_\phi$  can be easily braked by the Lorentz forces without any significant pressure increase. In the inviscid approximation, and considering only the  $m = 0$  mode of the Lorentz force, we end up with the ordinary differential equation for the Lorentz force induced perturbation  $\delta v_\phi(r, z)$  of the azimuthal velocity component:

$$\bar{v}_z(r, z) \frac{\partial}{\partial z} \delta v_\phi(r, z) = \frac{1}{\mu_0 \rho} [(\nabla \times \mathbf{B}) \times \mathbf{B}]_\phi(r, z) \quad (2)$$

In contrast to the procedure described in [19,27] where we had utilized the measured Joule power at a given supercriticality to calibrate the Lorentz force on the r.h.s of Eq. (2), here we solve Eq. (2) simultaneously with the induction equation. Note that Eq. (2) is solved both in the innermost channel where it describes the downward braking of  $v_\phi$ , as well as in the back-flow channel where it describes the upward acceleration of  $v_\phi$ . Both effects lead to a reduction

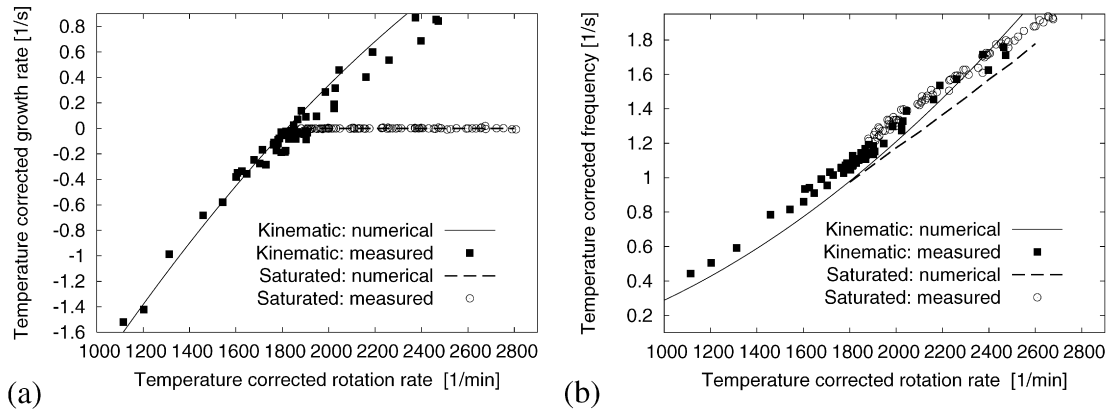


Fig. 4. Measured and computed growth rates (a) and frequencies (b) in the kinematic and saturated regime.

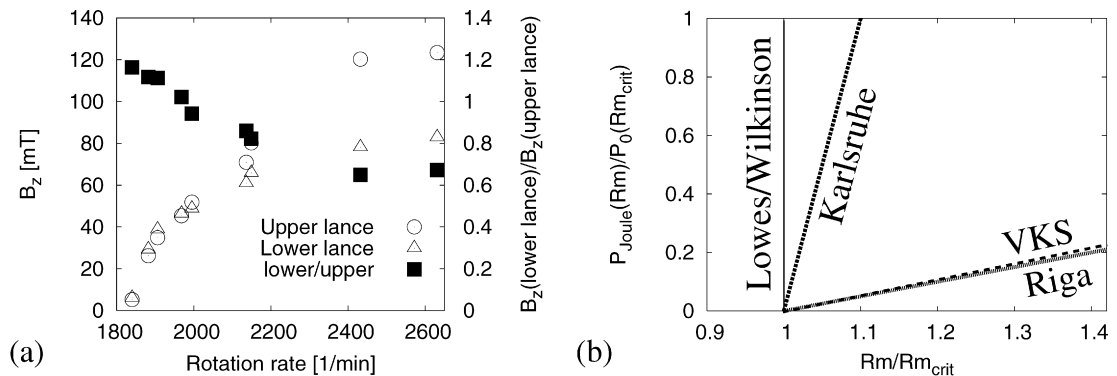


Fig. 5. (a) Decreasing ratio of fields at magnetic field sensors at the lower and upper lances. (b) The difference between experimental dynamos manifests itself in the steepness of the Joule power curve beyond the critical  $Rm_c$ . The more flexible a dynamo is, the easier it can refrain from producing more magnetic field.

of the differential rotation and hence to a deterioration of the dynamo capability of the flow. The validity of this self-consistent back-reaction model, which gives automatically a zero growth rate, can be judged from the dependence of the resulting eigenfrequency in Fig. 4(b). Actually, we see a quite reasonable correspondence with the measured data, in particular with respect to the slope of the curve. A slight jump of the measured eigenfrequencies between the kinematic and the saturated regime could be attributed to the arising fluid rotation in the outermost cylinder, which is not described by the back-reaction model according to Eq. (2). Other criteria for the quality of the back-reaction models are the correspondence of the resulting amplitude and shape of the eigenfield which also turned out to be quite satisfactory.

The braking of the azimuthal velocity component, which accumulates downstream from the propeller, results in a deteriorated self-excitation capability of the flow in the lower parts of the dynamo and therefore in an upward shift of the magnetic field structure. This is visible in Fig. 5(a) which shows the measured axial magnetic field amplitudes (from the June 2002 campaign) at the upper and lower ports and their ratio in dependence on the supercriticality. Corresponding dependencies for the outer Hall sensors were already documented in Fig. 12 of [20].

This deformation of the flow field under the influence of the Lorentz force of the self-excited magnetic field has a strong impact on the dependence of dissipated Joule power on the supercriticality. In Fig. 5(b) we try to compare the corresponding curves for the Loves and Wilkinson experiment [23], the Karlsruhe experiment [24], the VKS experiment [25], and the Riga experiment. Deliberately, we have given only a schematic plot of these dependencies since all four curves are not very accurately known. For the Loves and Wilkinson case we refer to their paper [23], for the Karlsruhe results we rely on the pressure increase shown in the inset of Fig. 4 in [24], for VKS we took the mean value between the estimates 15 and 20 per cent for a supercriticality of 30 per cent [25], for Riga we took the

fit  $P_{\text{Joule}} = (\Omega - 1840 \text{ rpm}) / (1840 \text{ rpm}) \times 48.4 \text{ kW}$  of the motor power measurements published in [27]. In stark contrast to the sharp rise for the Lowes and Wilkinson experiment, but also strongly differing from the steep increase in the Karlsruhe experiment, the Joule power dependence on supercriticality in both the VKS and the Riga experiment is very flat. For the latter we had already seen that, quite different to the back-reaction of a rigid body, the sodium flow deforms under the influence of the Lorentz forces, and the resulting deterioration of the dynamo condition makes the growth rate drop down to zero.

#### 4. Conclusions

The Riga dynamo experiment, which relies on the concept of the Ponomarenko dynamo, was the first successful liquid metal experiment in which the critical magnetic Reynolds number had been exceeded. Its kinematic regime has been simulated by a 2D-dimensional finite-difference solver with an accuracy of a few percent, and its saturated regime is qualitatively well understood by means of a simplified one-dimensional back-reaction model that accounts for the downward braking of the azimuthal component of the flow. The detailed measurements of the spatial structure of the magnetic eigenfield in dependence on the supercriticality make the Riga dynamo an ideal test-field for validating various MHD-turbulence models in a contemporary three-dimensional RANS model [28–30].

Contrary to what is sometimes written in the literature, the Riga dynamo has a highly unconstrained flow: the volume fraction in which the fluid flow is directly imposed by the propeller or by guiding blades is only 10 percent of the free flow volume behind the propeller. Interestingly, this is the same 10 per cent ratio as in the VKS experiment, hence it is not surprising that the slope of the Joule power curve is approximately the same in both experiments (see Fig. 5(b)). In contrast to the VKS experiment, the turbulence level in the Riga experiment is rather low (approximately 8%, depending on the position). The good correspondence of numerical predictions (based on the mean flow) with experimental data indicates that fluctuations of this level do not play a significant role in the dynamo mechanism.

A drawback of the Riga dynamo could be seen in the fact that it is definitely not suited for any investigation of field reversals since it is an oscillatory dynamo from the very outset. By virtue of its flow topology (a s1t1 in the terminology of Dudley and James [31]) there is no chance to observe any reversal process which, we believe, is connected with a transition between steady and oscillatory eigenvalues of the non-selfadjoint dynamo operator [32]. Such reversal studies have to be left to dynamo experiments with other flow topologies, e.g. of the s2t2 type as in the VKS experiment, in which reversals were actually observed [33].

The Riga dynamo is still operating. Further improvements of the velocity and magnetic field measuring techniques are planned and will possibly help to constrain turbulence models of flows under the influence of a self-excited magnetic field.

#### Acknowledgements

A significant number of people were involved in the construction of the facility and in carrying out the experimental campaigns. In particular, we are grateful to Arnis Cifersons, Sergej Dement'ev, Janis Zandarts, Anatolii Zik, Michael Christen, Heiko Hänel, and Gotthard Will.

We thank the Latvian Science Council for support under Grants Nos. 96.0276 and 01.0502, the Deutsche Forschungsgemeinschaft for support under INK 18/A1-1 and SFB 609, and the European Commission for support under HPRI-CT-2001-50027 and 028679.

#### References

- [1] P. Chossat, D. Armbruster, I. Oprea (Eds.), *Dynamo and Dynamics, A Mathematical Challenge*, Springer, Berlin, 2001.
- [2] K.-H. Rädler, *Magnetohydrodynamics* 38 (1–2) (2002).
- [3] A. Gailitis, O. Lielausis, E. Platācis, G. Gerbeth, F. Stefani, *Rev. Mod. Phys.* 74 (2002) 973–990.
- [4] A. Tilgner, *Astron. Nachr.* 323 (2002) 407–410.
- [5] A. Gailitis, O. Lielausis, G. Gerbeth, F. Stefani, *Dynamo experiments*, in: S. Molokov, et al. (Eds.), *Magnetohydrodynamics – Historical Evolution and Trends*, Springer, Berlin, 2007, pp. 37–54.
- [6] F. Pétrélis, N. Mordant, S. Fauve, *Geophys. Astrophys. Fluid Dyn.* 101 (2007) 289–323.
- [7] Yu.B. Ponomarenko, *J. Appl. Mech. Tech. Phys.* 14 (1973) 775–779.
- [8] M. Morris, K. Uchida, T. Do, *Nature* 440 (2006) 308–310.

- [9] A. Shukurov, D.D. Sokoloff, Hydromagnetic dynamo in astrophysical jets, in: *Cosmic Dynamo*, in: IAU Symposia, vol. 157, Kluwer, Dordrecht, 1993, pp. 367–371.
- [10] A. Gailitis, Ya. Freibergs, *Magnetohydrodynamics* 12 (1976) 127–129.
- [11] A. Gailitis, Ya. Freibergs, *Magnetohydrodynamics* 16 (1980) 116–121.
- [12] A. Gailitis, B.G. Karasev, I.R. Kirillov, O.A. Lielausis, S.M. Luzhanskii, A.P. Ogorodnikov, G.V. Preslitskii, *Magnetohydrodynamics* 23 (1987) 349–353.
- [13] A. Gailitis, *Magnetohydrodynamics* 32 (1996) 58–62.
- [14] F. Stefani, G. Gerbeth, A. Gailitis, Velocity profile optimization for the Riga dynamo experiment, in: A. Alemany, Ph. Marty, J.P. Thibault (Eds.), *Transfer Phenomena in Magnetohydrodynamic and Electroconducting Flows*, Kluwer, Dordrecht, 1999, pp. 31–44.
- [15] J.B. Taylor, *Rev. Mod. Phys.* 58 (1986) 741–763.
- [16] M. Christen, H. Hänel, G. Will, Entwicklung der Pumpe für den hydrodynamischen Kreislauf des Rigaer “Zylinderexperimentes”, in: W.H. Faragallah, G. Grabow (Eds.), *Beiträge zu Fluidenergiemaschinen 4*, Faragallah-Verlag und Bildarchiv, Sulzbach/Ts., 1998, pp. 111–119.
- [17] A. Gailitis, O. Lielausis, S. Dement’ev, E. Platadis, A. Cifersons, G. Gerbeth, Th. Gundrum, F. Stefani, M. Christen, H. Hänel, G. Will, *Phys. Rev. Lett.* 84 (2000) 4365–4368.
- [18] A. Gailitis, O. Lielausis, E. Platadis, G. Gerbeth, F. Stefani, *Magnetohydrodynamics* 37 (2001) 71–79.
- [19] A. Gailitis, O. Lielausis, E. Platadis, S. Dement’ev, A. Cifersons, G. Gerbeth, Th. Gundrum, F. Stefani, M. Christen, G. Will, *Magnetohydrodynamics* 38 (2002) 5–14.
- [20] A. Gailitis, O. Lielausis, E. Platadis, G. Gerbeth, F. Stefani, *Surv. Geophys.* 24 (2003) 247–267.
- [21] A. Gailitis, O. Lielausis, E. Platadis, S. Dement’ev, A. Cifersons, G. Gerbeth, Th. Gundrum, F. Stefani, M. Christen, G. Will, *Phys. Rev. Lett.* 86 (2001) 3024–3027.
- [22] A. Gailitis, O. Lielausis, E. Platadis, F. Stefani, G. Gerbeth, Laboratory astrophysics as exemplified by the Riga dynamo experiment, in: R. Rosner, G. Rüdiger, A. Bonanno (Eds.), *MHD Couette flows – Experiments and Models*, in: AIP Conference Proceedings, vol. 733, AIP, Melville, NY, 2004, pp. 35–44.
- [23] I. Wilkinson, *Geophys. Surveys* 7 (1984) 107–122.
- [24] R. Stieglitz, U. Müller, *Magnetohydrodynamics* 38 (2002) 27–33.
- [25] R. Monchaux, et al., *Phys. Rev. Lett.* 98 (2007) 044502.
- [26] A. Gailitis, O. Lielausis, E. Platadis, G. Gerbeth, F. Stefani, *Magnetohydrodynamics* 38 (2002) 15–26.
- [27] A. Gailitis, O. Lielausis, E. Platadis, G. Gerbeth, F. Stefani, *Phys. Plasmas* 11 (2004) 2838–2843.
- [28] S. Kenjereš, K. Hanjalić, S. Renaudier, F. Stefani, G. Gerbeth, A. Gailitis, *Phys. Plasmas* 13 (2006) 122308.
- [29] S. Kenjereš, K. Hanjalić, *Phys. Rev. Lett.* 98 (2007) 104501.
- [30] S. Kenjereš, K. Hanjalić, *New J. Phys.* 9 (2007) 306.
- [31] M.L. Dudley, R.W. James, *Proc. R. Soc. Lond. A* 425 (1989) 407–429.
- [32] F. Stefani, G. Gerbeth, *Phys. Rev. Lett.* 94 (2005) 184506.
- [33] M. Berhanu, *Europhys. Lett.* 77 (2007) 59001.